J Nanopart Res (2024) 26:119
https://doi.org/10.1007/s11051-024-06011-5

RESEARCH

Optimized wet-chemical synthesis of ultra-small CuO nanoparticles with high antibacterial activity

Xin-Yu Wang · Yan-Ming Chen · Xiao-Bo Nie · Li-Li Zhang

Received: 3 February 2024 / Accepted: 1 May 2024 / Published online: 30 May 2024

Abstract Copper oxide nanoparticles (CuO NPs) are attractive owing to their size- and shape-dependent properties, as well as their diverse applications. Therefore, the synthesis of environmentally friendly CuO NPs using low-toxicity reagents remains significant. In this study, a benign wet-chemical process was applied to synthesize CuO NPs in an alcohol-water mixture, employing copper acetate as the precursor and sodium oleate as the surfactant. Multiple experimental parameters, including water content, the molar ratio of sodium oleate to copper acetate, types of alcohols, and reaction temperature, were investigated to examine their effects on the formation and structures of the resulting products. Results from X-ray diffraction (XRD) and transmission electron microscopy (TEM) confirmed the monoclinic crystalline structure of CuO NPs with an ultra-small size of less than 3 nm. The size of CuO NPs can be easily adjusted by altering the water content, the molar ratio of precursor to surfactant, and other factors. The as-synthesized CuO NPs exhibited significantly enhanced antibacterial activity against *Escherichia coli* (*E. coli*) and *Staphylococcus aureus* (*S. aureus*).

Keywords Antibacterial properties · Copper oxide · Sodium oleate · Wet-chemical synthesis · X-ray diffraction (XRD)

X.-Y. Wang · Y.-M. Chen (✉) · L.-L. Zhang
School of Petrochemical Engineering, Shenyang University of Technology, Liaoyang (111003), Liaoning, China
e-mail: yanmchen@163.com

X.-B. Nie (✉)
College of Chemistry and Chemical Engineering, University of South China, Hengyang, Hunan (421001), China
e-mail: niexiaobo0101@163.com

Introduction

Copper oxide nanoparticles (CuO NPs) with distinctive physical and chemical properties have garnered significant attention not only for fundamental scientific research but also for various practical applications, including catalysis [1], photocatalysis [2], gas sensors [3], lithium-ion batteries (LIBs) [4], field emission displays (FEDs) [5], biological sensing and targeting [6], antibacterial agents [7, 8], and others [9]. In particular, copper, as an essential element in organisms, can be easily absorbed. Due to their good biocompatibility, heat resistance, antibacterial properties, and low biotoxicity, CuO NPs, representing copper-based materials, have been widely used as antibacterial materials [10–16]. Recent efforts have focused on fabricating nanostructured CuO to improve its performance in existing applications. However, the challenges in controlling the reaction, high preparation costs, and large particle sizes in the current preparation methods hinder the further application of CuO NPs. The persistent scientific pursuit and challenge is to prepare ultra-small CuO NPs,

which have consistently shown better performance than larger ones.

Currently, the preparation of CuO NPs involves both physical and chemical methods. Physical methods, such as laser cauterization [17], pulse electron deposition [18], and vacuum evaporation condensation [19], are commonly used to produce high-purity CuO products. However, the procedure requires very complicated and expensive equipment, and the production efficiency is low. Chemical methods for producing CuO NPs include solid-phase thermal conversion of precursors [20], the hydrothermal method [21, 22], the wet-chemical approach [23–25], the sol–gel method [26], the microwave technique [27], and chemical precipitation [28]. These methods enable the large-scale production of CuO NPs and greatly improve production efficiency. Moreover, the size, shape, and morphology of the resulting CuO NPs can be conveniently controlled. In particular, the wet-chemical approach is widely considered an important method for realizing the industrialization of nanomaterials. There are numerous advantages to prepare CuO NPs using the wet-chemical method, including the relatively simple process, controllable experimental parameters, the uniformity of resulting CuO NPs, small size, and controllable morphology. For instance, Dahonog et al. [25] successfully synthesized copper oxide nanostructures (Cu_2O and CuO) by adjusting the pH in a glycolic medium. Cubic Cu_2O NPs were formed under acidic conditions, while monoclinic CuO NPs were obtained in a basic solution. Nikam and colleagues [29] demonstrated a novel and scalable method for synthesizing CuO NPs with controllable shape and size by changing the concentration of the copper precursor. The production rate of CuO NPs was found to be 5 $g{\cdot}h^{-1}$, with 70% conversion of copper acetate into CuO NPs. While the wet-chemical method for synthesizing nanoparticles offers numerous advantages, it also has some drawbacks, including low purity of the resulting NPs and extended preparation time. It is necessary to choose the appropriate preparation method and process conditions based on specific preparation requirements and actual circumstances. To date, the controlled synthesis of nanostructured CuO with various sizes, shapes, and structures remains a prominent topic in nanoscience and nanotechnology.

Additionally, CuO NPs as the typical antibacterial agent have demonstrated excellent antibacterial activity against various bacterial strains, including *Escherichia coli* (*E. coli*), *Pseudomonas aeruginosa*, *Klebsiella pneumoniae*, *Enterococcus faecalis*, *Shigella flexneri*, *Salmonella Typhimurium*, *Proteus vulgaris*, *Bacillus subtilis*, and *Staphylococcus aureus* (*S. aureus*) [10, 14, 27, 30]. Among them, *Escherichia coli*, a common intestinal bacterium, can cause intestinal infections, diarrhea, and even lead to serious illnesses such as septicemia and meningitis. *Staphylococcus aureus*, a common bacterium found on the skin and in the respiratory tract, can cause a variety of diseases, such as skin infections, pneumonia, endocarditis, and food poisoning. It is important and necessary to prevent and control the presence and the number of *E. coli* and *S. aureus* for human health. It has been reported that the toxicity of CuO NPs towards *Escherichia coli* is attributed to complexation-mediated leaching by amino acids. The leached copper peptide complex caused a significant increase in intracellular reactive oxygen species (ROS) production and decreased the proportion of viable cells, leading to an overall inhibition of biomass growth. The authors emphasized the toxicity of CuO at the nanoscale [31].

Herein, CuO NPs were prepared in an alcohol-water mixture by the wet-chemical route, using copper acetate as the precursor and sodium oleate as the surfactant. The addition of a trace of water is crucial for the formation of CuO NPs, and the size of CuO NPs can be effectively controlled by adjusting the water content. The molar ratio of sodium oleate to copper acetate, the type of alcohols used, and the reaction temperature were investigated to determine their effects on the formation, size, and distribution of the resulting nano-products. With Gram-negative *E. coli* and Gram-positive *S. aureus* bacteria as model microorganisms, the as-synthesized CuO NPs exhibited significantly size- and concentration-dependent bactericidal effects.

Experimental section

Materials

Copper acetate ($Cu(CH_3COO)_2$, purity ≥ 98.0%), sodium oleate ($C_{17}H_{33}COONa$, purity > 97.0%), sodium hydroxide (AR, purity ≥ 99.5%), anhydrous ethanol (purity ≥ 99.5%), n-butanol (AR, 99%), and

hexyl alcohol (AR, 99%) were all purchased from Shanghai Aladdin Biochemical Technology Co. Ltd. Gram-negative *Escherichia coli* (*E. coli*) and Gram-positive *Staphylococcus aureus* (*S. aureus*) were obtained from the China Center of Industrial Culture Collection. The nutrients, including Luria broth (LB) medium and LB Agar, were sourced from Beijing Aoboxing Universeen Bio-Tech Co. Ltd. Secondary distilled water was obtained from the Power Plant of Liaoyang Petrochemical Company. All chemicals were used as received without further purification.

Synthesis of CuO NPs

A simple wet-chemical method was used to synthesize CuO NPs by using copper acetate as the precursor and sodium oleate as the surfactant in an ethanol–water mixture. Typically, 76 mg (0.25 mmol) of sodium oleate and 98 mL of anhydrous ethanol were first added to a three-necked reaction flask and heated to 80 °C under magnetic stirring to form an optically clear solution. Next, a fresh 0.25 $mol{\cdot}L^{-1}$ copper acetate aqueous solution (2 mL) was slowly added to the three-necked flask at a constant temperature of 80 °C. Raw materials were reacted at a constant temperature for half an hour. Here, the concentrations of sodium oleate and copper acetate in the reaction system, denoted as $[C_{17}H_{33}COONa]$ and $[Cu^{2+}]$, were 2.5×10^{-3} $mol{\cdot}L^{-1}$ and 5.0×10^{-3} $mol{\cdot}L^{-1}$, respectively. In the following parallel experiments, the total volume (100 mL) and the concentration of copper acetate ($[Cu^{2+}]=5.0\times10^{-3}$ $mol{\cdot}L^{-1}$) in the solvent mixture were kept the same. Several experimental factors, such as reaction temperature, water content (volume fraction), molar ratio of sodium oleate to copper acetate ($[C_{17}H_{33}COONa]$:$[Cu^{2+}]$), and types of alcohols, were monitored to study their impact on the formation, structure, and performance of the resulting CuO NPs. In contrast, CuO NPs were synthesized without a surfactant in an ethanol–water mixture with varying water content (2–8%).

After the reaction, the system was cooled to room temperature and left for a period to allow the precipitates to form completely. The precipitates were washed with ethanol using centrifugation (4000 rpm, 3 min for three times) and decantation operations to remove excess surfactant, unreacted precursor, and impurities. The purified CuO NPs were ultimately dried into powder for further testing.

Antibacterial assay

The antibacterial activity of CuO NPs was tested against *E. coli* and *S. aureus* bacterial strains using the agar well diffusion method. All culture dishes and materials were sterilized in an autoclave for 30 min before experiments. The bacterial suspension was incubated in Luria–Bertani (LB) medium using an orbital shaker at 37 °C to obtain isolated colonies. Freshly grown bacteria were cultured until the optical density reached 0.5 (approximately 10^9 colony-forming units (CFU) per milliliter). The bacteria in the logarithmic phase were collected by centrifugation at 4000 rpm for 5 min and then re-suspended in a 0.9% (w/v) saline solution for subsequent antibacterial experiments. The LB Agar plates were prepared and swabbed using a sterile inoculation ring with cultured bacterial strains. CuO NPs were dispersed in water by ultrasonic oscillation, and a certain amount of bacteria in a nutrient medium was added to sterile Petri plates to assess the activity of the CuO NPs. The plates were then incubated at 37 °C for 24 h, and the zone of inhibition, representing the activity of CuO NPs, was measured in millimeters (mm).

Characterization

Powder X-ray diffraction (XRD) is commonly used to analyze the phase composition and structure of crystals. XRD patterns of the prepared samples were recorded on a Rigaku SmartLab SE (Japan) diffractometer equipped with graphite monochromatized Cu Kα ($\lambda=1.54178$ Å) radiation. The scanning speed was set at 2°/min within the range of 20 to 90°. The voltage of 40 kV and operating current of 30 mA were used, respectively. Transmission electron microscopy (TEM) is commonly used in materials science to determine the size, shape, morphology, and dispersion of samples. Here, TEM measurements were conducted using a JEOL JEM-2010 instrument with an accelerating voltage of 100 kV. The TEM sample was prepared by depositing a single drop of CuO NPs solution in ethanol onto a 300-mesh carbon-coated copper grid.

Results and discussion

The synthesis of CuO NPs without surfactants

We used a simple and convenient wet-chemical method to synthesize CuO NPs. Briefly, the copper acetate aqueous solution and anhydrous ethanol were mixed and heated to 80 °C or higher to obtain CuO NPs. In the ethanol–water system, the water content plays an important role in the formation and size control of CuO NPs. CuO NPs cannot be obtained in the absence of water, but they are formed in the presence of water. A significant study by Chen [32] has also demonstrated the crucial role of water in the synthesis of pure CuO NPs in a water–ethanol solvent. With the assistance of water, copper acetate undergoes hydrolysis to form copper hydroxide ($Cu(OH)_2$), which then transforms into CuO either directly or indirectly (Eqs. (1), (2), and (3)).

$$\mathrm{Cu}\left(CH_3COO\right)_2 + 2H_2O \rightleftharpoons Cu(OH)_2 + 2CH_3\mathrm{COOH} \quad (1)$$

$$Cu(OH)_2 \rightarrow CuO + H_2O \quad (2)$$

$$Cu(OH)_2 + 2OH^- \rightleftharpoons Cu(OH)_4{}^{2-} \rightarrow CuO + H_2O + 2OH^- \quad (3)$$

Figure 1a shows XRD patterns of CuO NPs synthesized without surfactants, but with varying water content ranging from 2 to 8% in an ethanol–water mixture. All XRD patterns of CuO NPs, regardless of water content, exhibit characteristic peaks that align well with the standard diffraction peaks from JPCDS Card No. 48–1548. No other peaks belonging to the impurities, such as copper acetate, $Cu(OH)_2$, and Cu_2O, are observed. These indicate the high purity of CuO NPs and the monoclinic crystalline structure. The sharp diffraction peak at a 2θ angle of 35.3° is attributed to the $(11\bar{1})$ and/or (002) planes of monoclinic CuO. The prominent diffraction peak at 38.4°corresponds to the (111) and/or (200) planes. Other distinct diffraction peaks at 2θ of 48.7°, 57.8°, 61.3°, 66.4°, and 75° are accurately indexed to the $(20\bar{2})$, (202), $(11\bar{3})$, $(31\bar{1})$, and (004) planes of monoclinic CuO. The characteristic diffraction peaks of CuO NPs become narrower and sharper with the increase in water content, indicating an increase in the size of CuO NPs. In fact, the prominent diffraction at 38.4° was more inclined to (111) planes. Derived from the half-height width of the (111) peaks in Fig. 1a and calculated using the Debye–Scherrer formula [33, 34], the average crystal sizes of CuO NPs synthesized in different water content (2–8%) are 4.1 nm, 4.5 nm, 5.0 nm, and 6.5 nm, respectively.

TEM and HRTEM images in Fig. 1b–e depict the size, morphology, distribution, and lattice arrangement of CuO NPs synthesized under varying water content. In general, CuO NPs maintain a dot-shaped morphology regardless of water content. The mean diameter of CuO NPs is estimated to be *ca.* 5 nm, which is consistent with the size calculated by XRD analysis. Due to the high surface free energy of small-sized CuO nanodots, these unstable particles tend to aggregate in order to reduce system energy and maintain thermodynamic stability. The HRTEM images clearly show adjacent lattice spacings of 0.252 nm (Fig. 1b) and 0.253 nm (Fig. 1c), which correspond well to the $(11\bar{1})$ or (002) planes of monoclinic-phase CuO. Lattice spacings of 0.232 nm (Fig. 1d) and 0.231 nm (Fig. 1e) agree with the (111) or (200) plane of the monoclinic CuO structure.

The formation of CuO NPs modified by sodium oleate

In order to enhance the long-term stability of CuO NPs, a surfactant was added to the synthesis system to study its impact on the formation, structure, and performance of the resulting products. Here, sodium oleate was used as the surfactant to modify the synthesized CuO NPs. Sodium oleate, reported as an inexpensive and efficient capping reagent, has been extensively used for the synthesis of silver [34, 35] and cadmium sulfide [36] nanocrystals in our previous publications. Figure 2a shows the XRD patterns of CuO NPs synthesized by using sodium oleate as the surfactant at varying water content, ranging from 2 to 8%, in an ethanol–water mixture. Regardless of the water content, the characteristic diffraction peaks are all in accordance with those of monoclinic CuO (JCPDS 48–1548). No redundant or impure signals are observed, indicating the high purity and crystallinity of the synthesized CuO NPs.

Compared to the peaks in Fig. 1a, the diffraction peaks in Fig. 2a appear somewhat broader, suggesting a smaller crystal size of sodium oleate-modified CuO NPs. According to the Debye–Scherrer formula, the average diameters obtained from the

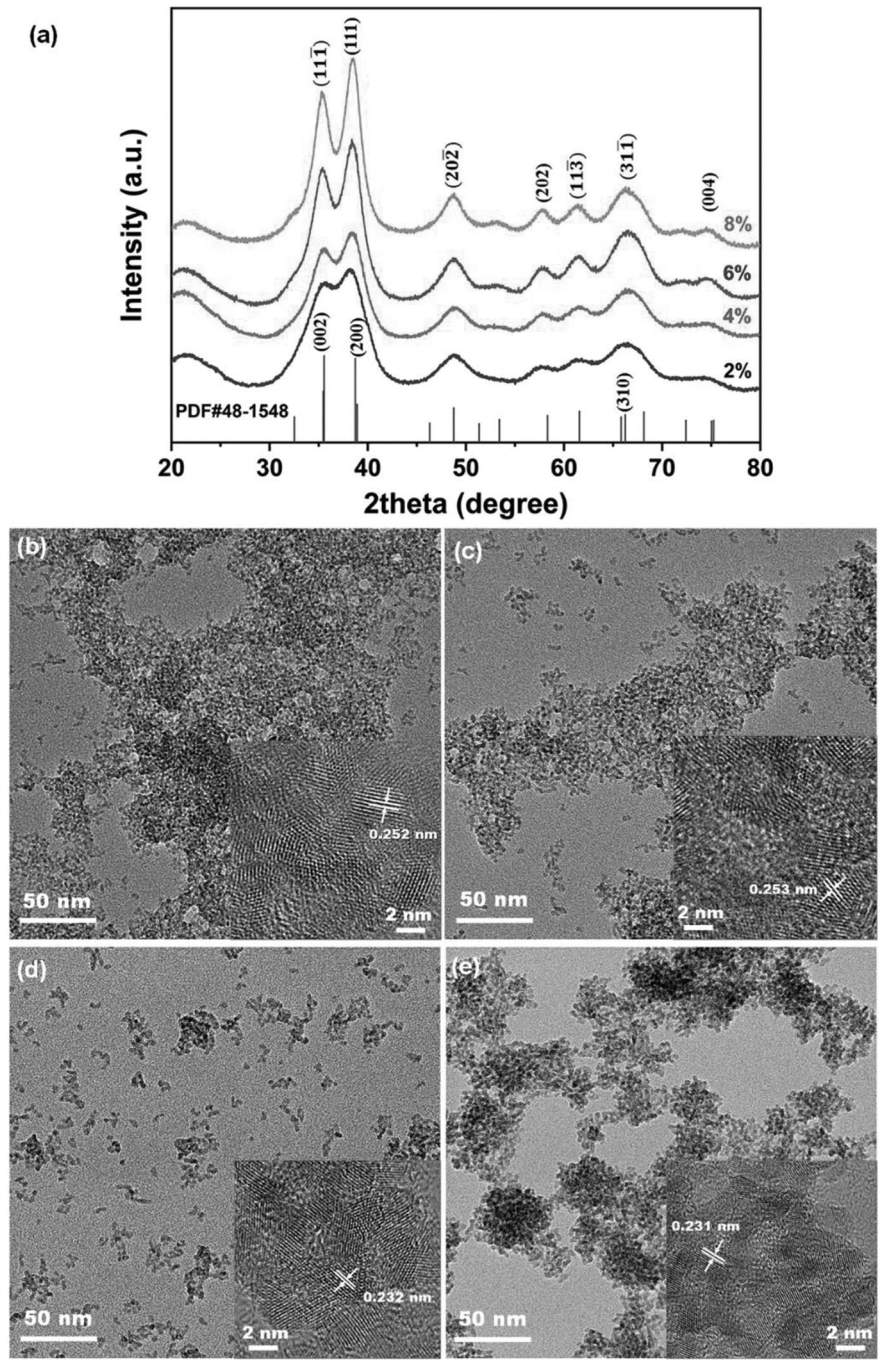

Fig. 1 **a** XRD patterns of CuO NPs prepared at different water content (2–8%) in an ethanol–water mixture and without surfactant. The corresponding TEM images show CuO NPs prepared in water contents of **b** 2%, **c** 4%, **d** 6%, and **e** 8%. HRTEM images in the lower right corners of **b**–**e** clearly show the arrangement of lattice planes

half-height width of the (111) peaks in Fig. 2a were calculated to be 2.85 nm, 3.59 nm, 3.70 nm, and 3.73 nm, corresponding to water content ranging from 2 to 8%. Evidently, the average crystal size of CuO NPs prepared using sodium oleate as the surfactant is quite smaller than that in the situation without surfactants. Therefore, sodium oleate is favorable for the formation of small-sized and high-purity CuO NPs. Furthermore, it is beneficial to obtain small-sized CuO NPs with a low water content (2%) in the ethanol–water mixture. Figure 2b–e displays TEM and HRTEM images of

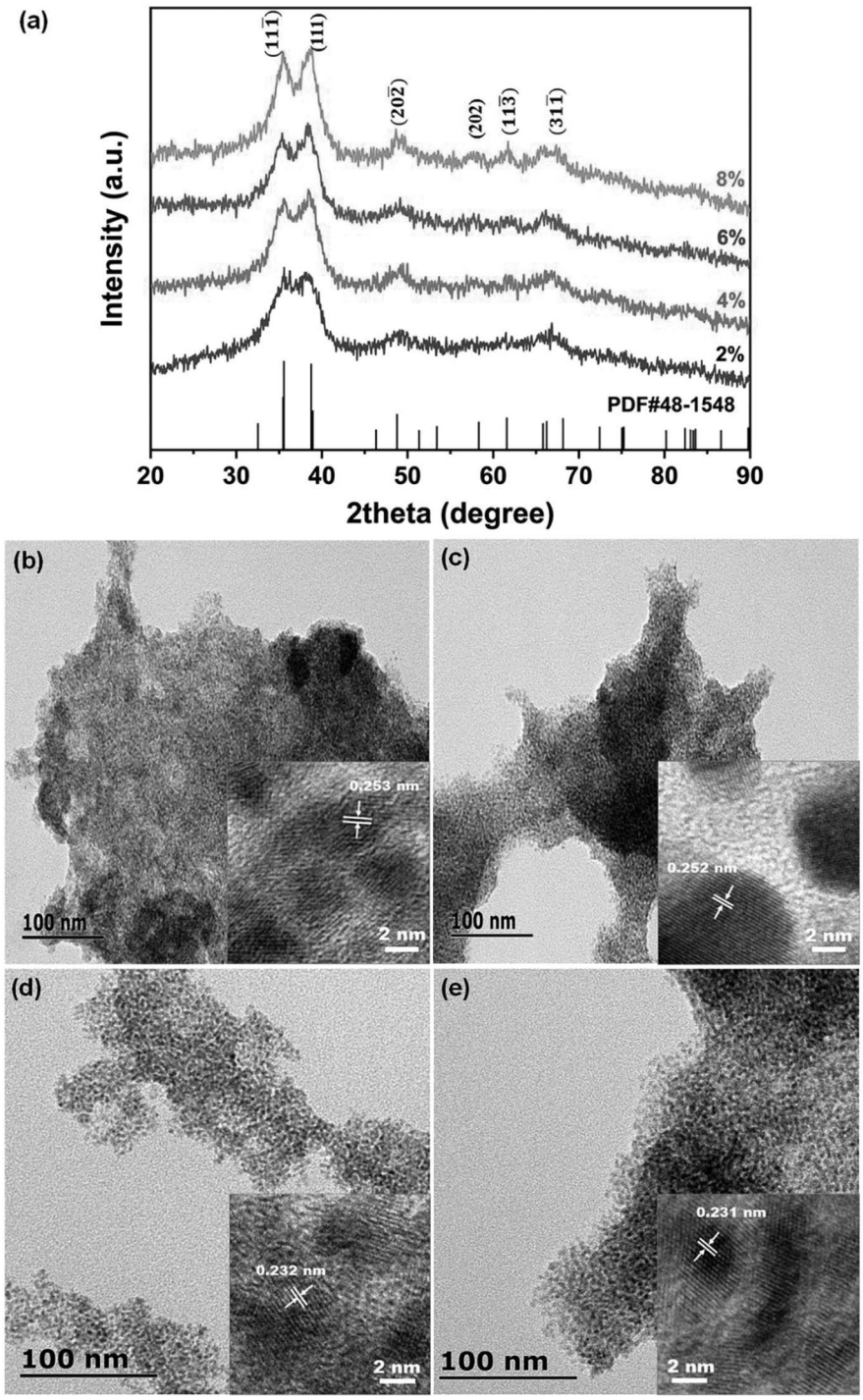

Fig. 2 **a** XRD patterns of CuO NPs prepared at different water content (2–8%) in an ethanol–water mixture and with sodium oleate as the surfactant. The corresponding TEM images show CuO NPs prepared in water contents of **b** 2%, **c** 4%, **d** 6%, and e 8%. HRTEM images in the lower right corners of **b**–**e** show clear arrangements of lattice planes

CuO NPs synthesized with water contents of 2%, 4%, 6%, and 8%, respectively. CuO NPs aggregate due to the low solubility of sodium oleate-modified CuO NPs in ethanol solvent. The distinct lattice arrangement and spacing in HRTEM images further demonstrate the crystalline structure of monoclinic CuO.

The effect of $[C_{17}H_{33}COONa]$:$[Cu^{2+}]$ on CuO NPs

In this section, we studied the effect of the additional amount of sodium oleate, denoted as $[C_{17}H_{33}COONa]$:$[Cu^{2+}]$, on the formation and structure of the resulting products. In the experiments, the concentration of copper acetate ($[Cu^{2+}]=5.0\times10^{-3}$ mol·L^{-1}) and the water content (2%) in the ethanol–water mixture remained constant, while the concentration of sodium oleate was varied. CuO NPs can be obtained under any conditions regardless of the $[C_{17}H_{33}COONa]$:$[Cu^{2+}]$ ratio (Fig. 3). The diffraction peaks in Fig. 3a correspond to the standard results of monoclinic CuO from JPCDS Card No. 48–1548. No redundant and impurity peaks are detected, indicating the high purity and crystallinity of the resulting CuO NPs. The diffraction peaks tend to become broader and flatter, and then narrow and sharpen as the $[C_{17}H_{33}COONa]$:$[Cu^{2+}]$ ratio increases. This demonstrates the size trend of CuO NPs, starting from large, then becoming small, and then returning to large.

According to the Debye–Scherrer formula, the mean diameters obtained from the half-height width of the (111) peaks in Fig. 3a are calculated to be 4.20 nm, 2.05 nm, 2.42 nm, and 3.58 nm, corresponding to the $[C_{17}H_{33}COONa]$:$[Cu^{2+}]$ ratios of 0.25:1, 0.5:1, 1:1, and 2:1, respectively. Especially, the ultra-small CuO NPs (2.05 nm) are prepared when the ratio of $[C_{17}H_{33}COONa]$ to $[Cu^{2+}]$ is 0.5. Therefore, the optimized molar ratio of sodium oleate to copper acetate was fixed at 0.5 for the formation of ultra-small CuO NPs in other parallel experiments. The TEM and HRTEM images in Fig. 3b–e reveal the agglomeration of CuO NPs due to their poor dispersion in ethanol, but they also show a visible lattice orientation, further demonstrating the presence of crystalline CuO NPs.

Preparation of CuO NPs in different alcohols

In the synthesis of CuO NPs in an alcohol-water solvent, alcohol, as the primary dispersion medium, may also play an additional role in the formation of CuO NPs. The varying polarity and viscosity of alcohols result in differential dissolution and diffusion of precursor and surfactant in the solvent. This facilitates control over the nucleation and growth of crystals, thereby regulating the size of CuO NPs. Here, n-butanol and hexyl alcohol were used as the dispersive solvents to respectively prepare CuO NPs with a water content of 2% and a $[C_{17}H_{33}COONa]$:$[Cu^{2+}]$ ratio of 0.5:1. Various reaction temperatures were monitored to study their effects on the formation and structure of the as-prepared CuO NPs. In the synthesis of CuO NPs in a mixture of n-butanol and water, XRD patterns (Fig. 4a), TEM and HRTEM images (Fig. 4b–e) confirm the generation of high-purity CuO NPs with a monoclinic crystalline structure. According to the Debye–Scherrer formula, the mean diameters derived from the half-height width of the (111) peaks in Fig. 4a are estimated to be 3.17 nm, 4.25 nm, 5.90 nm, and 6.36 nm, corresponding to reaction temperatures of 80 °C, 90 °C, 100 °C, and 110 °C, respectively. Thus, adjusting the reaction temperature offers an additional method for conveniently controlling the size of CuO NPs. The reaction temperature should be adjusted within the appropriate range. A temperature that is too low cannot initiate the reaction of precursors. Excessively high reaction temperatures may lead to uncontrolled nucleation and/or growth of nanocrystals, and even Oswald ripening [37], resulting in larger nanoparticle sizes and a wider size distribution.

Furthermore, hexyl alcohol, which has a higher boiling point and viscosity than n-butanol, was used as the dispersing solvent to investigate its impact on the formation and structure of CuO NPs. Similar to the previous studies, XRD (Fig. 5a), TEM and HRTEM (Fig. 5b–d) were applied to characterize the morphology, structure, size, and size distribution of the resulting products. Figure 5a shows XRD patterns of samples prepared in a hexyl alcohol-water mixture at different reaction temperatures. It is evident that CuO NPs exhibit characteristic diffraction peaks corresponding to the data from JPCDS No. 48–1548, which can be obtained at temperatures of 100 °C or higher. The average sizes of CuO NPs, as calculated using the Debye–Scherrer formula, are 6.45 nm and 7.84 nm, corresponding to reaction temperatures of 100 °C and 120 °C, respectively. CuO NPs are not produced at 80 °C, probably because the hydrolysis of copper acetate (as shown in Eq. (1)) is inhibited by the high boiling point and viscosity of hexyl alcohol. In summary, the size of CuO NPs increased with higher reaction temperatures and/or increased viscosity of the dispersing solvent.

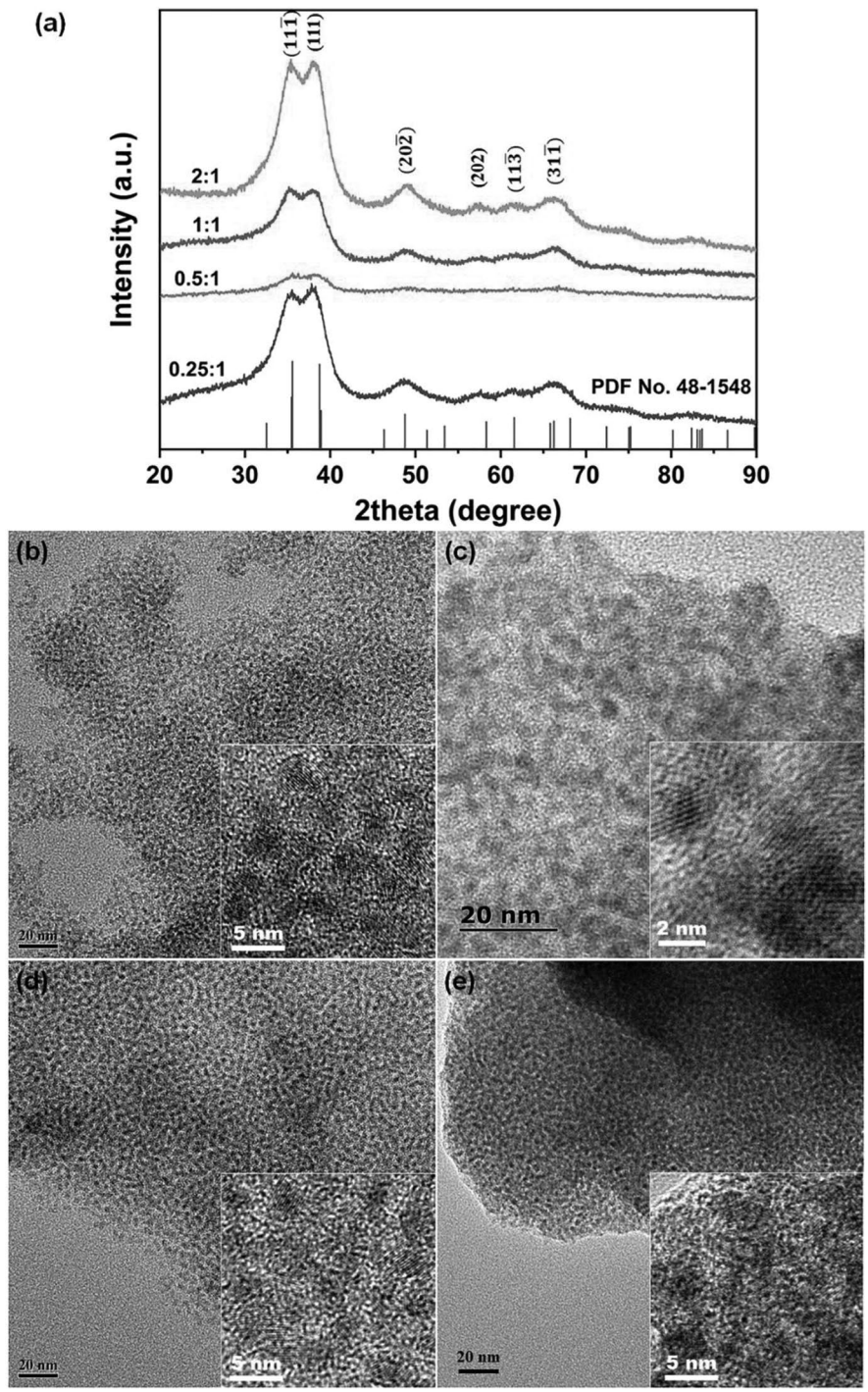

Fig. 3 **a** XRD patterns of CuO NPs prepared by varying the molar ratio of sodium oleate to copper acetate ([C H COONa]:[Cu]) from 0.25:1 to 2:1 in an ethanol–water system. The corresponding TEM images of CuO NPs prepared at the [C H COONa]: [Cu] ratios of **b** 0.25:1, **c** 0.5:1, **d** 1:1, and **e** 2:1. HRTEM images in the lower right corners in **b**–**e** display the distinct arrangement of lattice planes

Antibacterial effects of CuO NPs

Gram-negative *E. coli* and Gram-positive *S. aureus* were selected as model microorganisms. The antibacterial activity of CuO NPs with different sizes, prepared by using sodium oleate as the surfactant in an ethanol–water mixture at varied water content (as described in "The formation of CuO

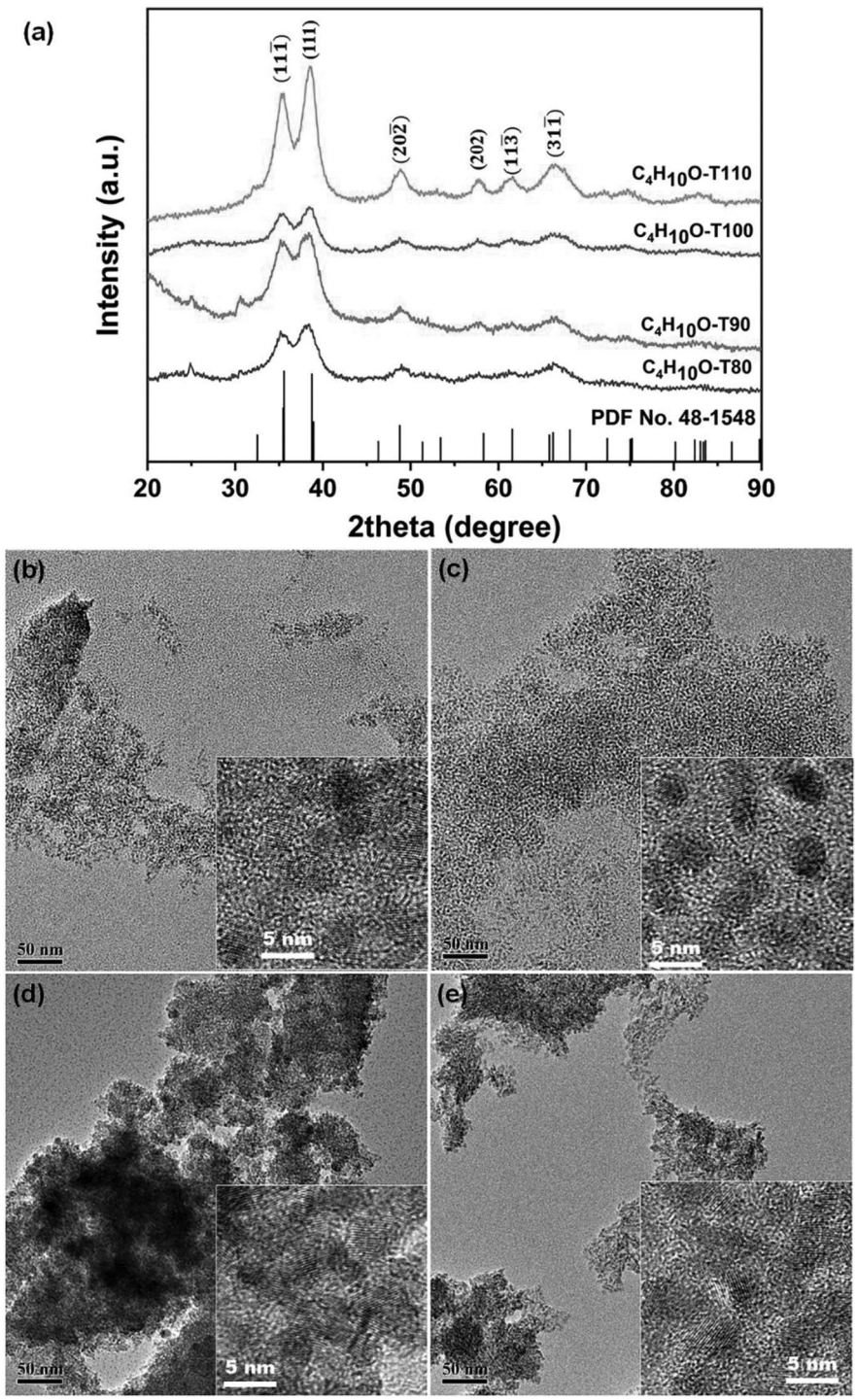

Fig. 4 **a** XRD patterns of CuO NPs prepared at different temperatures ranging from 80 to 110 °C in a mixture of n-butanol and water (2% volume fraction). The corresponding TEM images of CuO NPs prepared at the different temperatures: **b** 80 °C, **c** 90 °C, **d** 100 °C, and **e** 110 °C. The lower right corners in **b**–**e** display the HRTEM images of the corresponding samples

NPs modified by sodium oleate"), was evaluated. Four CuO samples with sizes of 2.85 nm, 3.59 nm, 3.70 nm, and 3.73 nm were synthesized at water contents of 2%, 4%, 6%, and 8%, respectively. The colony numbers of *E. coli* and *S. aureus* decreased, and the zones of inhibition significantly increased with the size increase of CuO NPs (Fig. 6). This study demonstrates the significant antibacterial

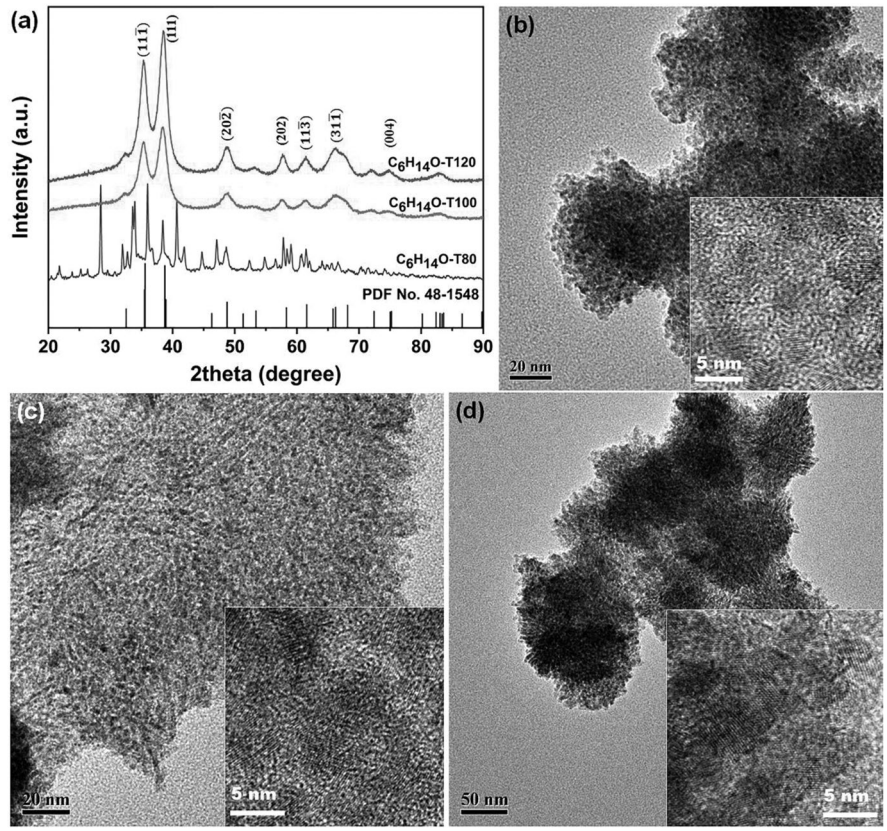

Fig. 5 **a** XRD patterns of CuO NPs prepared at different temperatures ranging from 80 to 120 °C in a mixture of hexyl alcohol and water (2% volume fraction). The corresponding TEM images show CuO NPs prepared at different temperatures: **b** 80 °C, **c** 100 °C, and **d** 120 °C. The lower right corners in **b**–**d** display the HRTEM images of the corresponding samples

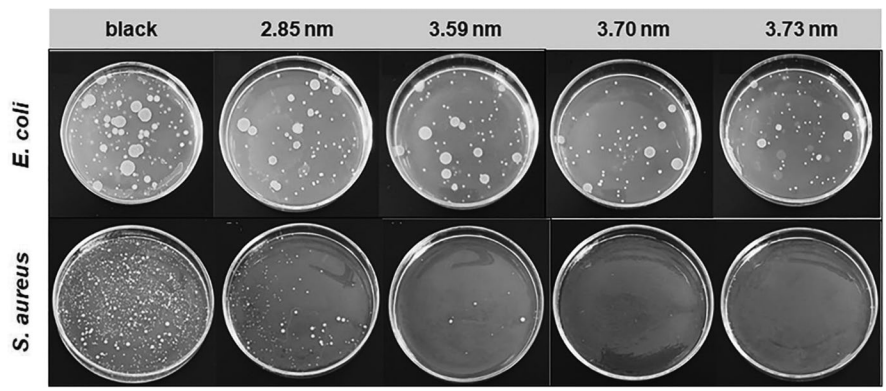

Fig. 6 Antibacterial photos of CuO NPs with various sizes synthesized in an ethanol–water system with different water content ranging from 2 to 8%, corresponding to sizes from 2.85 to 3.73 nm. The upper exhibits antibacterial effects against *Escherichia coli* at a concentration of 6×10^{-3} mol·L^{-1}. The lower shows the antibacterial effects on *Staphylococcus aureus* at the concentration of 1×10^{-3} mol·L.$^{-1}$

effect of CuO NPs against *E. coli* and *S. aureus*. The antibacterial effect is highly dependent on the size of CuO NPs. When exposed to CuO NPs, *S. aureus* was more sensitive than *E. coli*. Uddin [38, 39] used other nanoparticles and found the similar phenomena. Their findings clearly showed that Bi_2S_3 NPs were more active against Gram-positive *S. aureus* than Gram-negative *E. coli*.

Table 1 Antibacterial contrast of different sized CuO NPs to E. coli and S. aureus

Size of CuO NPs	E. coli		S. aureus	
	Average number of colonies	Antibacterial efficiency (%)	Average number of colonies	Antibacterial efficiency (%)
No CuO NPs	31	-	65	-
2.85 nm	17.5	43.5	3	95.4
3.59 nm	12.5	59.7	3	95.4
3.70 nm	6	80.6	0	100
3.73 nm	4.5	85.5	0	100

The process of biosorption of heavy metals by bacterial cells depends not only on the type of metal used but also on the microbial species being tested [30]. The inherent toxicity of metal oxide NPs and the specific type of bacteria are associated with the species' sensitivity to metal oxide NPs. The data listed in Table 1 clearly show that the antibacterial activity of CuO NPs improved with increasing nanoparticle size. The antibacterial efficiency of 3.73 nm-sized CuO NPs against *E. coli* can reach 85.5%, while the antibacterial efficiency against *S. aureus* can reach 100% at a lower concentration of CuO NPs (1×10^{-3} mol·L^{-1}). The high antibacterial efficiency is attributed to the small size and high surface activity of CuO NPs. Moreover, the variation in cell wall thickness and peptidoglycan layers between these two types of bacteria results in distinct antibacterial activity of CuO NPs. The thick cell wall and multiple layers of peptidoglycan in Gram-positive bacteria may hinder the penetration of agents, leading to a decrease in antibacterial activity. However, abundant amine and carboxylic functional groups on the surface of Gram-positive bacterial cells can bind with copper ions on the surface of CuO NPs, facilitating the entrance of CuO NPs into the cells of S. aureus [40]. Copper ions may also bind to DNA molecules of bacteria due to their high capacity to disrupt the helical structure. Thus, copper ions significantly disrupt the biochemical processes inside the bacterial cell [41]. In addition, the oxygen released on the surface of the CuO NPs can react with water molecules to form H_2O_2, which can penetrate inside and potentially kill these microorganisms [31].

Conclusion

A straightforward wet-chemical method was applied to synthesize CuO NPs in an alcohol-water mixture, employing copper acetate as the precursor and sodium oleate as the surfactant. The crystalline structure, size, and morphology of CuO NPs were characterized by XRD, TEM, and HRTEM. Experimental results showed that the addition of a trace amount of water was crucial for the formation of CuO nanocrystals. The size of CuO NPs increased with higher water content. The size of the as-synthesized CuO NPs in the presence of sodium oleate as the surfactant was smaller than in the absence of surfactant. Thus, reducing the water content and using a surfactant were advantageous for preparing ultra-small CuO NPs (< 3 nm). Other experimental parameters, such as the molar ratio of precursor to surfactant, reaction temperature, and types of alcohols, were also studied to investigate their effects on the formation, structure, and properties of the resulting products. The size of CuO NPs can be easily controlled by adjusting the parameters mentioned above. CuO NPs demonstrated significant size- and concentration-dependent antibacterial effects when targeting *E. coli* and *S. aureus*. CuO NPs exhibited a stronger inhibitory effect against *S. aureus* than against *E. coli*. In a significant finding, the antibacterial effectiveness of CuO NPs against *E. coli* and *S. aureus* increased as the size of the CuO NPs increased.

Author contribution Xin-Yu Wang performed the experiment and contributed to manuscript preparation; Yan-Ming Chen contributed to the conception and experimental design; Xiao-Bo Nie performed the data analyses and wrote the manuscript; Li–Li Zhang helped to perform the analysis with constructive discussions.

Funding This work was supported by the Key Project of Science and Technology Research from Department of Education of Liaoning Province (LJKZ0162).

Data availability Data sets generated during the study are available from the corresponding author on reasonable request.

Declarations

Competing interests The authors declare no competing interests.

Consent for publication Not applicable.

Conflict of interest The authors declare that they have no competing interests.

References

1. Baranov O, Bazaka K, Belmonte T, Riccardi C, Roman HE, Mohandas M, Xu S, Cvelbar U, Levchenko I (2023) Recent innovations in the technology and applications of low-dimensional CuO nanostructures for sensing, energy and catalysis. Nanoscale Horiz 8:568–602
2. Gawande MB, Goswami A, Felpin F-X, Asefa T, Huang X, Silva R, Zou X, Zboril R, Varma RS (2016) Cu and Cu-based nanoparticles: synthesis and applications in catalysis. Chem Rev 116:3722–3811
3. Steinhauer S (2021) Gas sensors based on copper oxide nanomaterials: a review. Chemosensors 9:51
4. Chai JL, Wang K, Li QM, Du JK, Jiang L, Han N, Zhang W, Tang BHJ, Rui YCA (2022) Highly dispersed CuO nanoparticle on ZIF-4 framework as anode material for LIBs. J Alloys Compd 914:165316
5. Lu CL, Chang SJ, Hsueh TJ (2018) Through-silicon submount for the CuO/Cu_2O nanostructured field emission display. RSC Adv 8:706–709
6. Verma N, Kumar N (2019) Synthesis and biomedical applications of copper oxide nanoparticles: an expanding horizon. ACS Biomater Sci Eng 5:1170–1188
7. Karim MN, Singh M, Weerathunge P, Bian P, Zheng R, Dekiwadia C, Ahmed T, Walia S, Della Gaspera E, Singh S, Ramanathan R, Bansal V (2018) Visible-light-triggered reactive-oxygen-species-mediated antibacterial activity of peroxidase-mimic CuO nanorods. ACS Appl Nano Mater 1:1694–1704
8. Ermini ML, Voliani V (2021) Antimicrobial nano-agents: the copper age. ACS Nano 15:6008–6029
9. Zhang Q, Zhang K, Xu D, Yang G, Huang H, Nie F, Liu C, Yang S (2014) CuO nanostructures: synthesis, characterization, growth mechanisms, fundamental properties, and applications. Prog Mater Sci 60:208–337
10. Das D, Nath BC, Phukon P, Dolui SK (2013) Synthesis and evaluation of antioxidant and antibacterial behavior of CuO nanoparticles. Colloids Surf B 101:430–433
11. Ren G, Hu D, Cheng EWC, Vargas-Reus MA, Reip P, Allaker RP (2009) Characterisation of copper oxide nanoparticles for antimicrobial applications. Int J Antimicrob Agents 33:587–590
12. Azam A, Ahmed AS, Oves M, Khan MS, Habib SS, Memic A (2012) Antimicrobial activity of metal oxide nanoparticles against Gram-positive and Gram-negative bacteria: a comparative study. Int J Nanomedicine 7:6003–6009
13. Azam A, Ahmed AS, Oves M, Khan MS, Memic A (2012) Size-dependent antimicrobial properties of CuO nanoparticles against Gram-positive and -negative bacterial strains. Int J Nanomedicine 7:3527–3535
14. Ahamed M, Alhadlaq HA, Khan MAM, Karuppiah P, Al-Dhabi NA (2014) Synthesis, characterization, and antimicrobial activity of copper oxide nanoparticles. J Nanomater 2014:637858
15. Meghana S, Kabra P, Chakraborty S, Padmavathy N (2015) Understanding the pathway of antibacterial activity of copper oxide nanoparticles. RSC Adv 5:12293–12299
16. Applerot G, Lellouche J, Lipovsky A, Nitzan Y, Lubart R, Gedanken A, Banin E (2012) Understanding the antibacterial mechanism of CuO nanoparticles: revealing the route of induced oxidative stress. Small 8:3326–3337
17. Rawat R, Tiwari A, Arun N, Rao SVSN, Pathak AP, Rao SV, Tripathi A (2020) Synthesis of CuO hollow nanoparticles using laser ablation: effect of fluence and solvents. Appl Phys A 126:226
18. Liguori A, Gualandi C, Focarete ML, Biscarini F, Bianchi M (2020) The pulsed electron deposition technique for biomedical applications: a review. Coatings 10:16
19. Djebian R, Boudjema B, Kabir A, Sedrati C (2020) Physical characterization of CuO thin films obtained by thermal oxidation of vacuum evaporated Cu. Solid State Sci 101:106147
20. Jia WZ, Reitz E, Sun H, Li B, Zhang H, Lei Y (2009) From $Cu_2(OH)_3Cl$ to nanostructured sisal-like $Cu(OH)_2$ and CuO: synthesis and characterization. J Appl Phys 105:064917
21. Zhu J, Bi H, Wang Y, Wang X, Yang X, Lu L (2008) CuO nanocrystals with controllable shapes grown from solution without any surfactants. Mater Chem Phys 109:34–38
22. Neupane MP, Kim YK, Park IS, Kim KA, Lee MH, Bae TS (2009) Temperature driven morphological changes of hydrothermally prepared copper oxide nanoparticles. Surface Interface Anal 41:259–263
23. El-Trass A, ElShamy H, El-Mehasseb I, El-Kemary M (2012) CuO nanoparticles: Synthesis, characterization, optical properties and interaction with amino acids. Appl Surf Sci 258:2997–3001
24. Hong Z-S, Cao Y, Deng J-F (2002) A convenient alcohothermal approach for low temperature synthesis of CuO nanoparticles. Mater Lett 52:34–38
25. Dahonog LA, Vega MSDCD, Balela MDL (2019) pH-dependent synthesis of copper oxide phases by polyol method. J Phys Conf Ser 1191:012043
26. Wang F, Li H, Yuan Z, Sun Y, Chang F, Deng H, Xie L, Li H (2016) A highly sensitive gas sensor based on CuO nanoparticles synthetized via a sol-gel method. RSC Adv 6:79343–79349
27. Kannan K, Radhika D, Vijayalakshmi S, Sadasivuni KK, Ojiaku A, Verma U (2022) Facile fabrication of CuO nanoparticles via microwave-assisted method: photocatalytic,

antimicrobial and anticancer enhancing performance. Int J Environ Anal Chem 102:1095–1108
28. Abhilasha KN, Gautam R (2023) Investigation of impact of pH and rare earth metal dopant concentration on structural, optical and thermal properties of CuO nanoparticles. Appl Phys A 129:64
29. Nikam AV, Dadwal AH (2019) Scalable microwave-assisted continuous flow synthesis of CuO nanoparticles and their thermal conductivity applications as nanofluids. Adv Powder Technol 30:13–17
30. Baek Y-W, An Y-J (2011) Microbial toxicity of metal oxide nanoparticles (CuO, NiO, ZnO, and Sb_2O_3) to Escherichia coli, Bacillus subtilis, and Streptococcus aureus. Sci Total Environ 409:1603–1608
31. Gunawan C, Teoh WY, Marquis CP, Amal R (2011) Cytotoxic origin of copper(II) oxide nanoparticles: comparative studies with micron-sized particles, leachate, and metal salts. ACS Nano 5:7214–7225
32. Chen L, Li L, Li G (2008) Synthesis of CuO nanorods and their catalytic activity in the thermal decomposition of ammonium Perchlorate. J Alloys Compd 464:532–536
33. Wani IA, Khatoon S, Ganguly A, Ahmed J, Ganguli AK, Ahmad T (2010) Silver nanoparticles: large scale solvothermal synthesis and optical properties. Mater Res Bull 45:1033–1038
34. Han J, Chen Y-M, Nie X-B (2022) Surface plasmon resonance of silver nanocrystals in ethylene glycol: regulation by multiple thermodynamic factors. J Clust Sci 34:2373–2380
35. Han J, Chen Y-M, Nie X-B (2020) Environmentally benign and large-scale synthesis of monodisperse oleate-protected silver nanoparticles in ethanol. J Clust Sci 32:899–905
36. Nie X-B, Chen Y-M (2021) Observation of dominant nuclei and magic-sized CdS nanoparticles in a single-phase system. J Nanosci Nanotechnol 21:5987–5992
37. Vetter T, Iggland M, Ochsenbein DR, Hänseler FS, Mazzotti M (2013) Modeling nucleation, growth, and Ostwald ripening in crystallization processes: a comparison between population balance and kinetic rate equation. Cryst Growth Des 13:4890–4905
38. Uddin I, Abzal SM, Kalyan K, Janga S, Rath A, Patel R, Gupta DK, Ravindran TR, Ateeq H, Khan MS, Dash JK (2022) Starch-assisted synthesis of Bi_2S_3 nanoparticles for enhanced dielectric and antibacterial applications. ACS Omega 7:42438–42445
39. Uddin I, Abzal SM, Kalyan K, Janga S, Patel R, Dash JK (2023) Starch-assisted stable synthesis of CdS nanoparticles for enhanced electrical and optical properties. J Electron Mater 52:1710–1716
40. Padil VVT, Cernik M (2013) Green synthesis of copper oxide nanoparticles using gum karaya as a biotemplate and their antibacterial application. Int J Nanomedicine 8:889–898
41. Camacho-Flores BA, Martínez-Álvarez O, Arenas-Arrocena MC, Garcia-Contreras R, Argueta-Figueroa L, de la Fuente-Hernández J, Acosta-Torres LS (2015) Copper: Synthesis techniques in nanoscale and powerful application as an antimicrobial agent. J Nanomater 2015:415238